Available Online at www.ijcsmc.com

International Journal of Computer Science and Mobile Computing

A Monthly Journal of Computer Science and Information Technology

ISSN 2320–088X
IMPACT FACTOR: 5.258

IJCSMC, Vol. 5, Issue. 3, March 2016, pg.550 – 559

Accelerometer Based Gesture Controlled Solar Energized Robot

Hemabrabha.G[1], Abishek.S[5], Madhumathi.P[2], Vignesh.S[3], Vikashini.K.M[4]
[1]Assistant Professor, Department of EEE, Info Institute of Engineering, Coimbatore-641107, India
[2,3,4,5] UG Student, Department of EEE, Info Institute of Engineering, Coimbatore-641107, India

[1] hemaprabhaeee@gmail.com, [2] madhumathieee2995@gmail.com, [3] vicky64694@gmail.com, [4] vikashiniviks@gmail.com, [5] abivel07@gmail.com

---

Abstract- Solar energy in particular is the wide range of energy utilized under the category of renewable energy for generating electri city. Many applications like hand held calculators, recreation of electronics, traffic lights and utilization of solar energy alone for irrigations has evolved. This energy has a problem with storage of harvested energy. This paper presents an idea of utilizing solar energy in the field of robotics. As robots are electro-mechanical devices they are normally battery draining in nature. To satisfy the power requirement of robot, interfacing solar panel with a battery would be a better choice. Robots working under the field of outdoors like military this technique can be emphasized. Here, the robot is controlled using gesture movement by sensing, coding and transmitting the signals. The robot (receiving end) alone is powered using solar panel interfaced battery. To this end, a solar powered gesture controlled robot is designed mathematically and tested at indoors using high power light sources.

Key words- "Accelerometer", "Gesture Controlled Robot", "Solar Panel", "Renewable energy energized robot", "Rover with solar panel".

I. INTRODUCTION

Due to increase in energy consumption and depletion of fossil fuels, the renewable energy sources have become rare. Nowadays solar and wind energy power generations are rapidly growing when compared to other renewable source. In India solar potential is high and wind power generations have the limitation of medium wind profile, low plant factor and saturation of optimal wind locations. Solar irradiation is abundant in India by figures (4 -7) kw/m^2 per day in all over the country with 300clear sunny days in a year. The 70% of Indian population are involved in agricultural and living in rural areas. Still 1/3rd of Indian population are not connected to grid electric supply for that reason photo voltaic distributed power generation is most popular. And that sort of energy if get utilized can solve more number of problems in dense populated countries like India. In this project solar power is utilized for the robot working under military, medicine, heavy industries etc which utilizes the solar energy to power up. As robots are usually electro-mechanical machines, they consume more energy for the movement of mechanical parts by means of electrical controllers. The replacement of utilizing renewable energy would make more convenient utilizations under remote areas.

First, the background information necessary to understand photovoltaic cell is presented and followed by the description about making of robot utilizing solar energy.

II. PHOTOVOLTAIC CELLS

The photovoltaic cells was first discovered by a French physicist, Edmund Becquerel, while experimenting with an electrolytic cell in his father's laboratory made up of two metal electrodes at 1839, at the age of 19. He observed that exposing the metals to sun light caused an increase in conductance. Nearly forty years later, a structure considered to be the first solar cell, with about 1% efficiency, was developed. More efficient photovoltaic cells weren't introduced until semiconductor materials were discovered. The efficiency of a cell is mainly a function of fabrication material, the junction and the electrical contacts [1].

Normally PV cells are manufactured using silicon. When P and N junction doped with impurities are joined together a depletion region is formed. When light hits this region photons are absorbed and they knock off this depletion region by separating electrons from holes. This increases the conduction of the material. When circuit is closed with a load current flows in that path to energize the load. Fig 1 depicts a common p-n junction diode. If an external bias is applied to the diode then it is called a photodiode and it operates in reverse bias. The total current in this case is given by equation (1) [2].

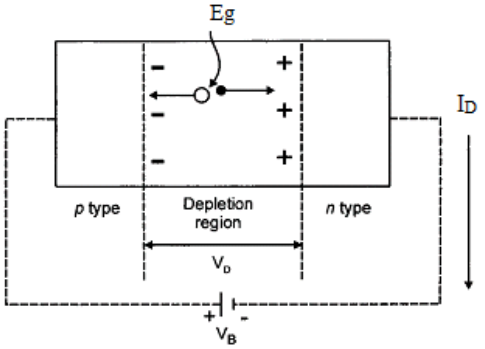

Fig.1 A p-n junction diode.

Therefore, a photovoltaic cell is characterized in terms of an open circuit voltage and short circuit current. The maximum power of a panel occurs under short circuit current and open circuit voltage condition. Once a load is attached to the cell, the maximum power is no longer at that bias point and it is the task of a designer to attempt to generate a maximum power condition in order to maximize efficiency. A single photovoltaic cell does not have a significant bias point at maximum power condition. To increase the power cells are combined into modules, and arrays.

A. Mathematical Modeling

The newly introduced concept is the utilization of solar energy from the solar panel [4,5]. Mathematical modeling of the solar panel is explained below based on the equivalent circuit of a PV cell, shown in Fig.2.

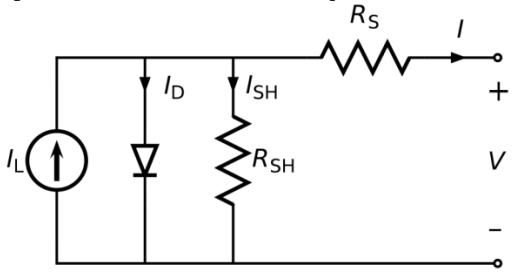

Fig.2 Equivalent circuit of a PV cell

$$I = I_L - I_D - I_{SH} \quad (1)$$

Five important equations to be considered are

1) Light-Generated Current (I_l)
2) Reverse Saturation Current (I_o)
3) Shape Factor (λ)
4) Series Resistance (R_s)
5) Output power (P_{max})

R_{SH} is considered to be very small in rating and hence its mathematical modeling is neglected [7].

Formulas Used to calculate the unknown important parameters

1) *Light-Generated Current (I_l):* The light-generated current (I_L) is a function of solar radiation and module temperature, if the series resistance (R_s) and shape factor (λ) are taken as constants. For any operating condition, I_L is related to the light-generated current measured at some reference conditions as [8,9]

$$I_L = (\frac{S_T}{S_{T,r}})[I_{L,r}+\mu I_{SC}(T_C-T_{C,r})] \quad (2)$$

2) *Reverse Saturation Current (I_o):* The reverse saturation current (I_o) is a function of temperature only[10].

$$I_o=(\frac{T_C}{T_{C,r}})^3 e^{\xi\lambda\varepsilon_g(T_{C,r}-T_C)/A} \quad (3)$$

3) *Shape Factor (λ):*Mostly, manufacturers provide information of I-V characteristics curve at three different point using reference conditions, at open circuit voltage (V_{oc}), at short circuit (I_{sc}), and at optimum power point for both the current and voltage. The correlation for the given points are I=0 and V=V_{OC} at open circuit conditions, I=I_{SC} and V=0 at short circuit conditions, and I=I_{mp} and V=V_{mp} at maximum power point [11]. By substituting these expressions in (1), it yields

$$I_{SC,r}=I_{L,r}-I_{o,r}[e^{(\xi_r I_{SC,r}R_S)}-1] \quad (4)$$

Where,

$$\xi_r=\frac{q}{\lambda k T_{C,r}} \quad (5)$$

$$I_{L,r}- I_{o,r}[e^{(\xi_r V_{OC,r})}-1]=0 \quad (6)$$

$$I_{mp,r}=I_{L,r}-I_{o,r}[e^{\xi_r(V_{mp,r}+I_{mp,r}R_S)}-1] \quad (7)$$

The reverse saturation current (I_o) is very small quantity on the order of 10^{-5} to 10^{-6} A [7]. It lessens the influence of the exponential term in (4). Hence, it is assumed to be equivalent to I_{SC} [3]. One more generalization can be made regarding the first term in (13) and (14), which could be ignored. Regardless of the system size, the exponential term is much greater than the first term. Thus, the equations become

$$I_{L,r}\cong I_{SC,r} \quad (8)$$

$$I_{SC,r}- I_{o,r}[e^{(\xi_r I_{SC,r}R_S)}] \cong 0 \quad (9)$$

$$I_{mp,r}\cong I_{L,r}- I_{o,r}[e^{\xi_r(V_{mp,r}+I_{mp,r}R_S)}] \quad (10)$$

Solving (9) for the reverse saturation current at reference conditions, ($I_{o,r}$) is obtained as

$$I_{o,r}= I_{SC,r}[e^{-(\xi_r V_{OC,r})}] \quad (11)$$

By substituting the value of reverse saturation current at reference conditions ($I_{o,r}$) from (11) into (10) , it yields

$$I_{mp,r}\cong I_{SC,r}- I_{SC,r}[e^{\xi_r(V_{mp,r}-V_{OC,r}+I_{mp,r}R_S)}] \quad (12)$$

Equation (10) can also be solved for ξ_r, which is given as

$$\xi_r=\frac{\ln(1-\frac{I_{mp,r}}{I_{SC,r}})}{V_{mp,r}-V_{OC,r}+I_{mp,r}R_s} \quad (13)$$

Finally the value of shape factor (λ) can be obtained by comparing (5) and (13) as

$$\lambda = \frac{q(V_{mp,r}-V_{OC,r}+I_{mp,r}R_S)}{kT_{C,r}\ln(1-\frac{I_{mp,r}}{I_{SC,r}})} \quad (14)$$

4) *Series Resistance (R_s):* The series resistance (R_s) is an essential parameter when the module is not operating near the reference conditions. This characterizes the internal losses due to current flow inside the each cell and in linkages between cells. It alters the shape of I-V curve near optimum power point and open circuit voltage as shown in fig 4.5.b. However, its effect is small . I-V curve without considering R_s would be somewhat dissimilar than the curves outlined including its value. On the basis of annual simulation, the predicted power output from PV system will be 5% to 8% lower when correct series resistance is not used. It can be determined as

$$\left.\frac{dV}{dI}\right|_{V_{OC}} - R_S = 0 \quad (15)$$

To obtain differential coefficient for (15), first the current (I) can be extracted explicitly as a function of voltage (V) by using Lambert W function from (7) and is expressed as

$$I=(I_L+I_o) - \frac{W\xi R_S e^{\xi(V+I_L R_S+I_o R_S)}}{\xi R_S} \quad (16)$$

By differentiating (16) with respect to V and taking its reciprocal at $V=V_{oc,r}$ and $I_L=I_{L,r}$ and substituting into (22), it gives

$$\frac{W(\xi R_S I_o e^{\xi(V_{OC,r}+I_{L,r}R_S+I_o R_S)})}{[1+W\left(\xi R_S I_o e^{\xi(V_{OC,r}+I_{L,r}R_S+I_o R_S)}\right)]R_S} - R_S = 0 \quad (17)$$

A number of simplifications have been made in order to solve (17) analytically for R_s. for example , I_o is usually taken in the order of 10^{-5} to 10^{-6} . Its value for this study was taken as the order of 10^{-6}. Similarly, the values of $I_{L,r}$ and $V_{oc,r}$ were taken from the manufacturers data. The expressions for R_s is obtained based on the above simplifications and by putting the value of ξ in (17) as

$$R_s = 1.8\ \mathrm{Re}\left[\frac{T_c W\left(-1.5\times10^7 e^{0.022\left(47+\left(1.7\times\frac{10^5}{T_c}\right)\right)}\right)}{T_c W\left(-1.5\times10^7 e^{0.022\left(47+\left(1.7\times\frac{10^5}{T_c}\right)\right)}\right)+4400}\right] \quad (18)$$

where Re represents the real part, because the negative expression inside the Lambert W function results in complex number. However, in practical problems only real values are to be considered.

5) *Output power (P_{max}):* The optimum power output parameters of model were determined by deriving the equations for current (*I*) and voltage (*V*) by putting the values of unknown parameters, namely, *IL*, *Io*, *R* and*λ*, in the respective equations. The power (*P*) is the product of current (*I*) and voltage (*V*)

$$P_{max}=\left\{(I_L+I_o)-\frac{W[\xi R_S e^{\xi[V_{max}+I_L R_S+I_o R_S]}]}{\xi R_S}\right\} \quad (19)$$

Where,

q - Electron charge 1.602×10^{-19}C
k - Boltzmann constant 1.381×10^{-23}J/K
$T_{c,r}$ - Cell temperature at actual conditioin,K
$V_{mp,r}$ - Maximum peak value of PV module reference,V
$I_{mp,r}$ - Maximum current value of PV module reference,A
$I_{sc,r}$ - Short circuit current of PV module reference,A
R_s - Series Resistance, Ω
$V_{oc,r}$ - Open circuit voltage of PV module reference,V
$S_{T,r}$ - Absorbed solar radiation reference,W/m^2
S_T - Absorbed solar radiation ,W/m^2
$I_{L,r}$ – Light- generated current reference,A
μ I_{SC} –Temperature coefficient of Short circuit current of PV module,A
T_C – Cell temperature at actual conditions,K
A - Ideality factor 1 for ideal diodes,between 1 and 2 for real diode
ξ - Parameter $q/KT_c\lambda$
ε_g - Material band gap energy,eV,1.12eV for silicon
W - Lambert W function
I_L - Light- generated current ,A
Io - Diode reverse saturation current,A

III. BLOCK DIAGRAM

The task is divided into two parts as shown in Fig.3 and Fig. 4. One is the transmitter session and another is receiver session. The transmitter end consists of an Accelerometer, Arduino Board, Encoder, Transmitter.

The accelerometer records the hand movement in X Y directions and outputs constant analog voltage levels. These potentials are fed to the microcontroller present in the Arduino UNO board. The displacement data is processed as per the program coded in the microcontroller and is sent after encoding to receiver part via transmitter RF module. The transmission is done in ASCII data exchange in RF modules.

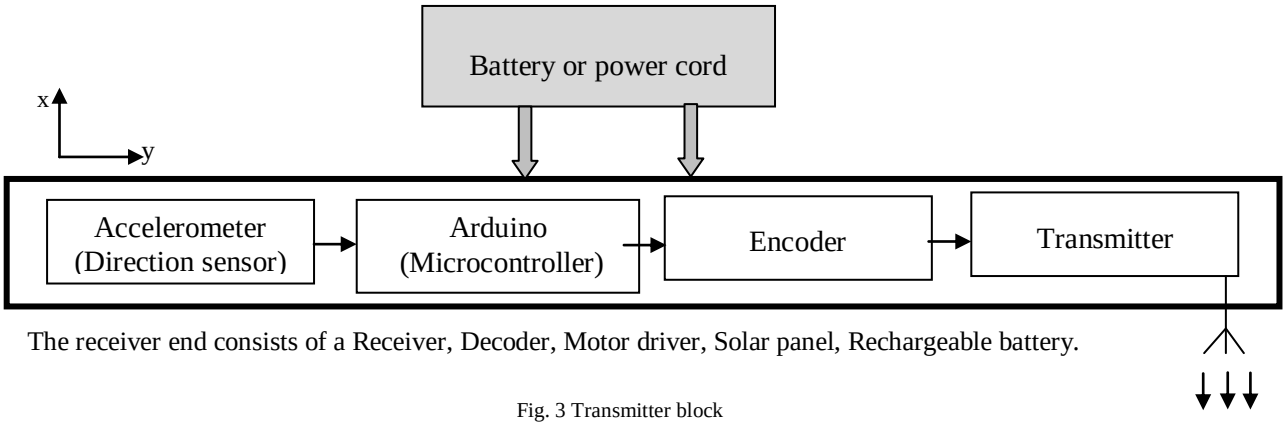

The receiver end consists of a Receiver, Decoder, Motor driver, Solar panel, Rechargeable battery.

Fig. 3 Transmitter block

On the receiver side the robot receives the RF signals and decodes it with the help of a decoder. The decoded signal has appropriate digital HIGH/LOW signals as per the program fed on the transmitter side and flows to the enable pins of DC motor driver. The solar panel is interfaced in battery for the charging of battery.

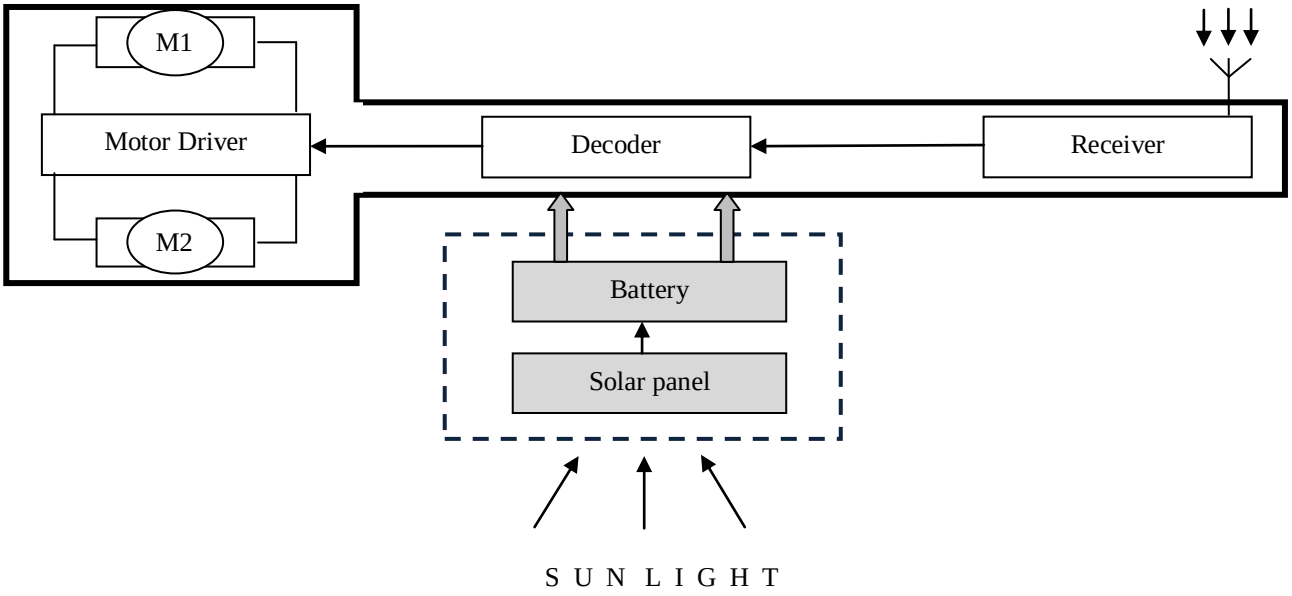

Fig. 4 Receiver Block

IV. EXPERIMENTAL DETAILS

Following are the major components used in gesture controlled robot

1) Accelerometer **(adxl335)**
2) Arduino UNO **(containing microcontroller atmega328)**
3) Encoder **(HT12E)**
4) 433MHz 4 channel RF pair
5) Rechargeable battery **(12V,1.3A, Pb acid non spillable)**
6) Motor Driver **(L293D)**
7) DC motor **(12V, 60 RPM)**
8) Solar Panel (Specifications are in Table I)

TABLE I
SOLAR PANEL SPECIFICATIONS

S.No	SPECIFICATION	RATING
1.	Maximum power (P max)	2.4 W
2.	Voltage at maximum power(V_{mpp})	12V
3.	Current at maximum power (Impp)	0.2A
4.	Open circuit Voltage (Voc)	14.4V
5.	Short circuit current (Isc)	0.22A
6.	Cells	144
7.	Plug fuse rating	0.5A
8.	Array	6×4
9.	Dimension	105×60×10mm

V. TRANSMITTING AND RECEIVING CIRCUITS

The transmitter circuit, shown in Fig.6 consists of an accelerometer (adxl335) which senses the displacement of made by the hand. This displacement is recorded in terms of potentials and is fed to Arduino UNO containing atmega328 microcontroller. Program based on the displacement produces the enable signals of DC motor which is on the receiver side. Now, the enable signals for the motor to rotate are ready and needs to be transmitted. Before transmitting the enable signals it needs to get encoded. Hence, HT12E encoder encodes the digital signal for transmitting. 4 channel 433 MHz RF pair is used for transmitting and receiving the radio frequency signals. This transmitter receiver module supports ASCII standard exchange of data.

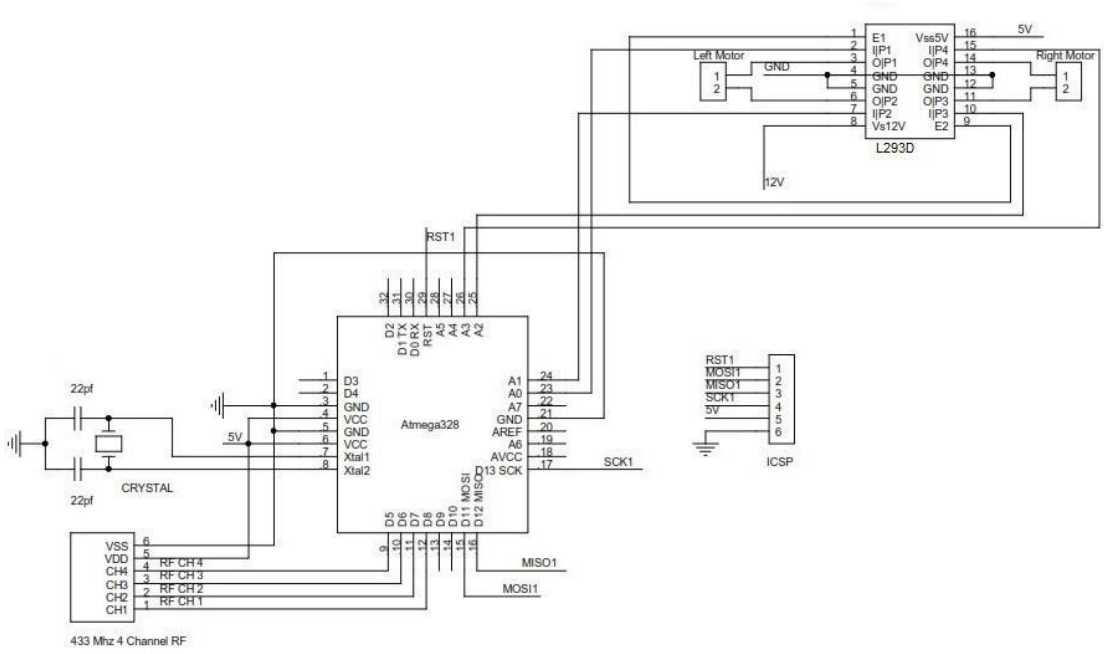

Fig. 6 Transmitter Circuit

The receiver circuit of robot, shown in Fig.7 consists of a 4 channel 433MHz receiver. The signal that is already programmed in the Arduino UNO which is on the sender circuit is received here. This signal needs to be decoded. Hence,

HT12D decoder is used to decode the signals received. This signal is given directly to the motor driver L293D in which there are two enable pins. Based on the digital signal whether it is high or low the motor rotates. L293D is configured in H bridge connection for clockwise and anti clockwise rotations which is explained in Fig.11. A H bridge is an electronic circuit that enables a voltage to be applied across a load in either direction. These circuits are often used in robotics and other applications to allow DC motors run forwards and backwards [6]

The solar panel is interfaced with battery on the receiver side i.e., on the robot. As the controller remains in safer area in a room the transmitter side is powered up using an adapter or a charged battery. The DC motors need 12V and IC chips need only 5 V hence for ICs a 7805 voltage regulator regulates the 12V potential to 5V and supplies the ICs. The circuit diagram in Fig. 6 and Fig. 7 is marked in labeling concept for clearance. A diode is placed in between battery and solar panel to prevent the back flow of current from the battery to solar panel.

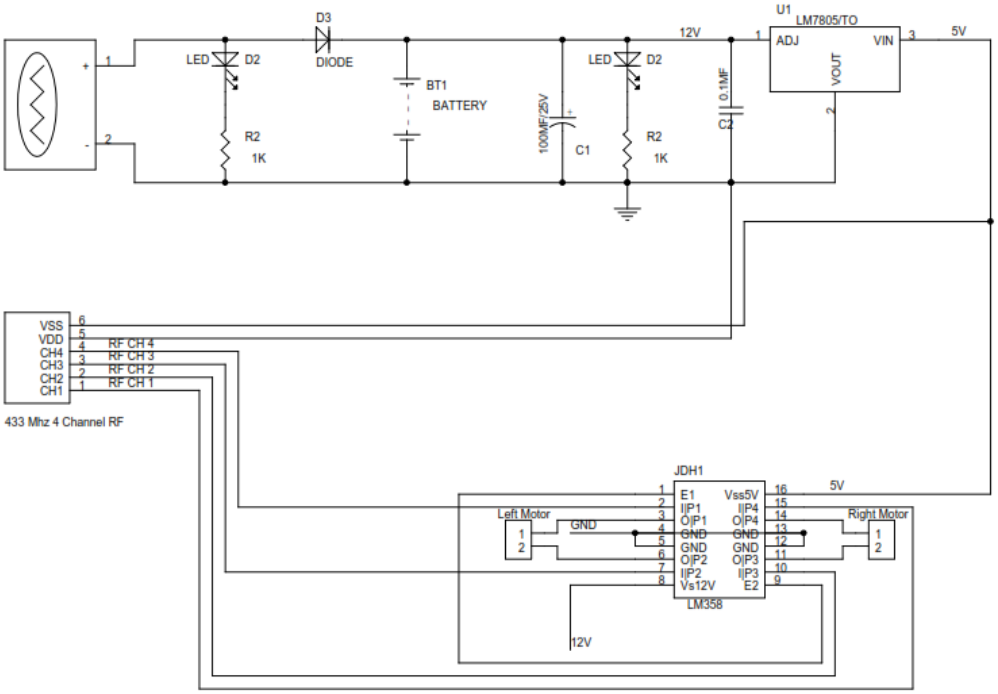

Fig. 7 Receiver Circuit

VI. SIMULATION

Solar panel simulation is done in MATLAB and Simulink, shown in Fig. 8 to obtain the VI and PI characteristics of the solar panel. The simulation is done by sensing current, voltage. The data obtained from the sensor is fed to PS-Simulink converters. This PS-Simulink converter converts the analog signals into physical data for plotting waveform and graphs. The output data of voltage and current is multiplied for obtaining the power of solar panel. These obtained data are calculated by means of formulas in configurations. The waveforms are obtained in I-V and P-V scopes which are shown in Fig. 9 and Fig. 10.

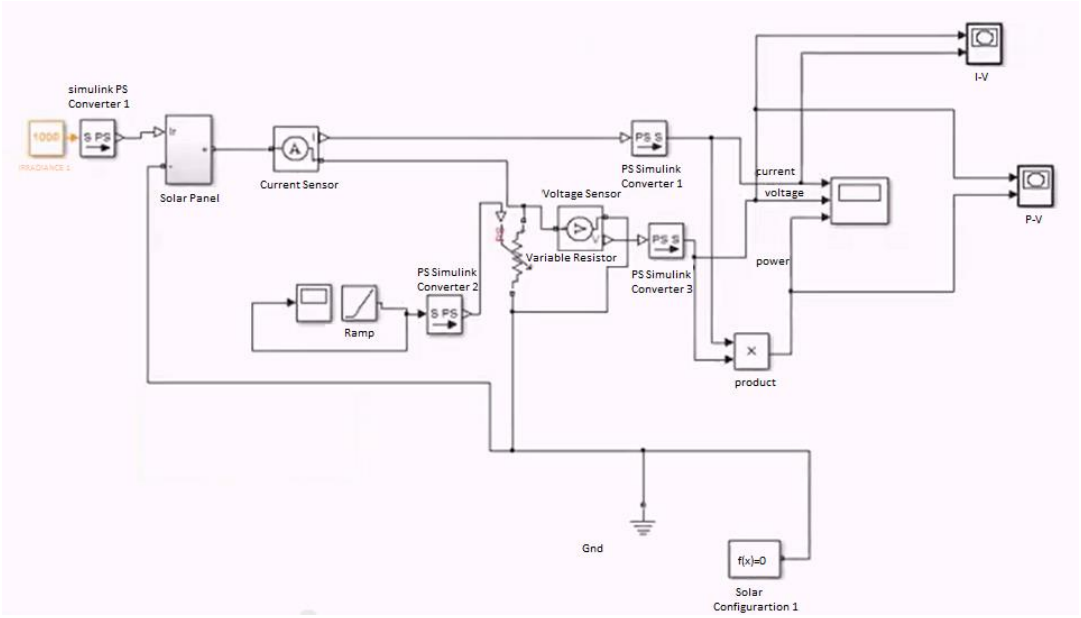

Fig. 8 Simulation of Solar Panel in MATLAB and Simulink

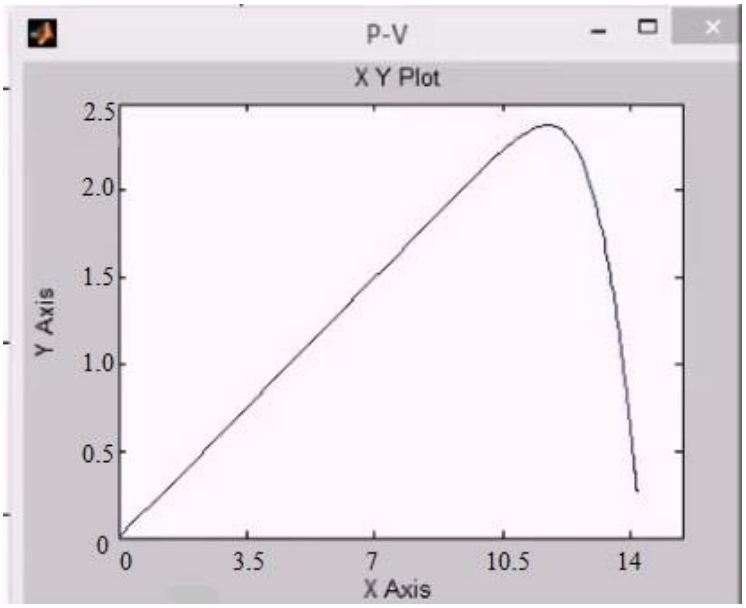

Fig. 9 Simulated Graph of PV module scope P-V (Power -Voltage characteristics)

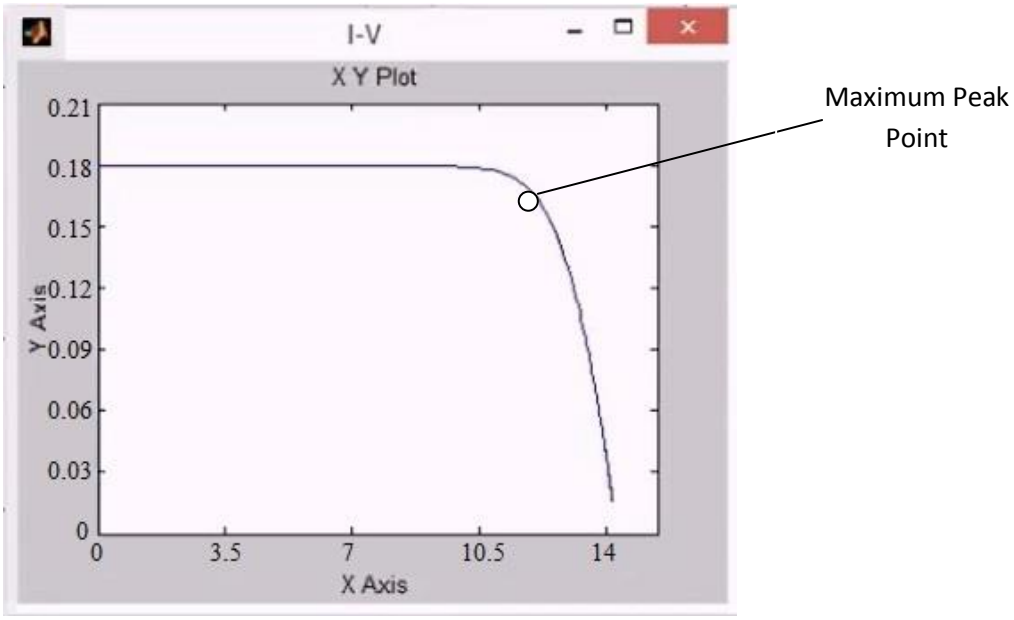

Fig. 10 Simulated Graph of PV module scope I-V (Current -Voltage characteristics)

The solar panel waveforms in I-V and P-V characteristics as shown in Fig.9 and Fig.10 are obtained from the scopes P-V and I-V in Fig. 8 in which I_{max} is nearly 0.2A, V_{max} is 12V and P_{max} is 12V. Which implies that the optimum power point of the solar panel characteristics lies at 12V,0.2A which covers more part of region when integrated. The selection of optimum power flow point is such a way that maximum area of V-I is covered for better production of power with minimum losses.

VII. CONCLUSION

The purpose of the project is to utilize the renewable energy for the movement of robot and conserve the non renewable energies for future generation. As robots generally have some electronic parts and more mechanical parts for movement they consume more energy for the mechanical parts and electronics as well. This energy demand for the robots cannot be supplied always with the already recharged battery or powering up through an adapter as wiring itself is a big disadvantage. This robot when equipped in the applications of military like detection of mines and dismantling them roves in sun light hence this gets charged effectively. This prevents the mental pressure for the controllers to notify the back up of battery and replacement under peak situations. Battery gets charged at the time of robots working time itself. Equatorial nations like India are always exposed to sun light over a wide area and seasonal changes have no recognizing impact over sun light intensity. Hence this can be used everywhere in the places of outdoor environment. This robot can be used in indoor also in the field of medicines for doing surgery etc by utilizing the stored energy from the battery in the situation of operating a spreadable diseased patients by Doctors. If this technique is improvised more non renewable energy can be saved for our future generation.

VIII. FUTURE SCOPE

1) As we are using RF for wireless transmission, the range is quite limited; nearly 60 m. this problem can be solved by utilizing a GSM module for wireless transmission. The GSM infrastructure installed almost all over the world. GSM will not only provide wireless connectivity but also quite a large range.

2) Secondly, an on-board camera can be installed for monitoring the robot from faraway places. All we need is a wireless camera which will broadcast and a receiver module which will provide live streaming.

3) Thirdly, this robot gets charged slowly from solar panel than its speed of getting drained. Hence we can either replace some alternate power source or replace the current DC motors with ones which require less power.

4) The robot is in its primary level using this idea the gesture controlled arms for pick and place of objects, mine detecting equipments mounted on with an arm to dismantle it in military and larger size of robots can be designed and implemented.

5) Instead of using batteries Super Capacitors can be used by combining capacitors one can achieve a higher current at constant voltage (parallel combination) or a higher voltage at constant current (series combination) [3]

REFERENCES

[1] Soares,A., "A Two-Color CMOS Optical Detector Circuit", Proceedings of IEEE SoutheastCon 2007, Richmond, VA., pp.562-565, March 2007.

[2] "An Improved Mathematical Model for Computing Power Output of Solar Photovoltaic Cells" Abdul Qayoom Jakhrani, Jane Labadin, Saleem Raza Samo and Andrew Ragai Henry Rigit Shakeel Ahmed Kamboh, Proceedings Hindawi Publishing Corporation, International Journal of Photoenergy Volume 2014, Article ID 346704.

[3] Boylestad, R,. "*Introductory Circuit Analysis* 11th Edition," Upper Saddle River, NJ: Pearson Education, Inc., 2007.

[4] W. Kim and W. Choi, "A novel parameter extraction method for the one-diode solar cell model," Solar Energy,vol.84,no.6,pp. 1008–1019, 2010.

[5] A. H. Fanney, B. P. Dougherty, and M. W. Davis, "Evaluating building integrated photovoltaic performance models," in Proceedings of the 29th IEEE Photovoltaic Specialists Conference (PVSC '02),NewOrleans,La,USA,May2002.

[6] Al Williams(2002). *Microcontroller projects using the Basic Stamp*, 2nd ed., Focal Press.p.344 ISBN 978-1-57820-101-3.

[7] R. L. Boylestad, L. Nashelsky, and L. Li, Electronic Devices and Circuit Theory,Prentice-Hall,10thedition,2009.

[8] A. Jain and A. Kapoor, "A new approach to study organic solar cell using Lambert W-function," Solar Energy Materials and Solar Cells,vol.86,no.2,pp.197–205,2005.

[9] W.DeSoto,S.A.Klein,andW.A.Beckman,"Improvementand validation of a model for photovoltaic array performance," Solar Energy,vol.80,no.1,pp.78–88,2006.

[10] J. Crispim, M. Carreira, and C. Rui, "Validation of photovoltaic electrical models against manufacturers data and experimental results," in Proceedings of the International Conference on Power Engineering, Energy and Electrical Drives zPOWERENG '07),pp. 556–561, Setubal, Portugal, April 2007.

[11] E.Saloux,A.Teyssedou,andM.Sorin,"Explicitmodelof photovoltaic panels to determine voltages and currents at the maximum power point," Solar Energy,vol.85,no.5,pp.713–

